Inorg. Chem. **2005**, *44*, 4756–4765

Controlled Hydrolysis of Lanthanide Complexes of the N-Donor Tripod Tris(2-pyridylmethyl)amine versus Bisligand Complex Formation

Louise Natrajan,[†] Jacques Pécaut,[‡] Marinella Mazzanti,*[,†] and Colette LeBrun[†]

Laboratoire de Reconnaissance Ionique and Laboratoire de Coordination et Chiralité, Service de Chimie Inorganique et Biologique, CEA/DSM/ Département de Recherche Fondamentale sur la Matière Condensée, CEA-Grenoble, 38054 Grenoble, Cedex 09, France

Received February 11, 2005

The reaction of the lanthanide salts $LnI_3(thf)_4$ and $Ln(OTf)_3$ with tris(2-pyridylmethyl)amine (tpa) was studied in rigorously anhydrous conditions and in the presence of water. Under rigorously anhydrous conditions the successive formation of mono- and bis(tpa) complexes was observed on addition of 1 and 2 equiv of ligand, respectively. Addition of a third ligand equivalent did not yield additional complexes. The mono(tpa) complex $[Ce(tpa)I_3]$ (**1**) and the bis(tpa) complexes $[Ln(tpa)_2]X_3$ (X = I, Ln = La(III) (**2**), Ln = Ce(III) (**3**), Ln = Nd(III) (**4**), Ln = Lu(III) (**5**); X = OTf, Ln = Eu(III) (**6**)) were isolated under rigorously anhydrous conditions and their solid-state and solution structures determined. In the presence of water, ^{1}H NMR spectroscopy and ES-MS show that the successive addition of 1–3 equiv of tpa to triflate or iodide salts of the lanthanides results in the formation of mono(tpa) aqua complexes followed by formation of protonated tpa and hydroxo complexes. The solid-state structures of the complexes $[Eu(tpa)(H_2O)_2(OTf)_3]$ (**7**), $[Eu(tpa)(\mu\text{-}OH)(OTf)_2]_2$ (**8**), and $[Ce(tpa)(\mu\text{-}OH)(MeCN)(H_2O)]_2I_4$ (**9**) have been determined. The reaction of the bis(tpa) lanthanide complexes with stoichiometric amounts of water yields a facile synthetic route to a family of discrete dimeric hydroxide-bridged lanthanide complexes prepared in a controlled manner. The suggested mechanism for this reaction involves the displacement of one tpa ligand by two water molecules to form the mono(tpa) complex, which subsequently reacts with the noncoordinated tpa to form the dimeric hydroxo species.

Introduction

The coordination chemistry of the lanthanides is receiving an increasingly large amount of attention due to the many important applications of lanthanide complexes in areas such as medicine, catalysis, and materials science.[1−4] Hydroxide ligands are of interest in lanthanide chemistry as reaction sites for condensation to bridged oxides[5] and as nucleophiles in RNA cleavage and in the catalytic hydrolysis of phosphate diesters.[6−16] Although the unambiguous identification of the active species is very difficult, it is indeed generally accepted that the catalysis of phosphate diester cleavage involves substrate activation by a dinuclear lanthanide core followed by nucleophilic attack by an activated hydroxide ligand. Recently the systematic preparation of sophisticated lan-

* Author to whom correspondence should be addressed. E-mail: mazzanti@drfmc.ceng.cea.fr.
[†] Laboratoire de Reconnaissance Ionique.
[‡] Laboratoire de Coordination et Chiralité.

(1) Kido, J.; Okamoto, Y. *Chem. Rev.* **2002**, *102*, 2357−2368.
(2) Parker, D.; Dickins, R. S.; Puschmann, H.; Crossland, C.; Howard, J. A. K. *Chem. Rev.* **2002**, *102*, 1977−2010.
(3) Bünzli, J.-C. G.; Piguet, C. *Chem. Rev.* **2002**, *10*, 1897−1928.
(4) Caravan, P.; Ellison, J. J.; McMurry, T. J.; Lauffer, R. B. *Chem. Rev.* **1999**, *99*, 2293−2352.
(5) Hubert-Pfalzgraf, L. G. *New J. Chem.* **1987**, *11*, 663−675.
(6) Huskens, J.; Kennedy, A. D.; B., H.; Peters, J. A. *J. Am. Chem. Soc.* **1995**, *117*, 375−382.
(7) Morrow, J. R.; Aures, K.; Epstein, D. *J. Chem. Soc., Chem. Commun.* **1995**, 2431−2432.
(8) Morrow, J. R.; Buttrey Lisa, A.; Shelton, V. M.; Berback, K. *J. Am. Chem. Soc.* **1992**, *114*, 1903−1905.
(9) Tsubouchi, A.; Bruice, T. C. *J. Am. Chem. Soc.* **1995**, *117*, 7399−7411.
(10) Williams, N. H.; Takasaki, B.; Wall, M.; Chin, J. *Acc. Chem. Res.* **1999**, *32*, 485−493.
(11) Sreedhara, A.; Cowan, J. A. *J. Biol. Inorg. Chem.* **2001**, *6*, 337−347.
(12) Ragunathan, K. G.; Schneider, H.-J. *Angew. Chem., Int. Ed. Engl.* **1996**, *35*, 1219−1221.
(13) Hurst, P.; Takasaki, B.; Chin, J. *J. Am. Chem. Soc.* **1996**, *118*, 9982−9983.
(14) Roigk, A.; Hettich, R.; Schneider, H.-J. *Inorg. Chem.* **1998**, *37*, 751−756.
(15) JureK, A. M.; Jurek, P. E.; Martell, A. E. *Inorg. Chem.* **2000**, *39*, 1016−1020.
(16) Bligh, A. S. W.; Choi, N.; Evagourou, E., G.; McPartlin, M.; White, K. N. *J. Chem. Soc., Dalton Trans.* **2001**, 3169−3172.

10.1021/ic0502224 CCC: $30.25
Published on Web 05/20/2005

Chart 1

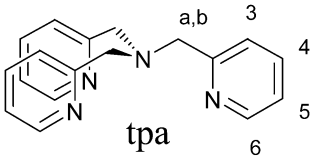

thanide oxo/hydroxo complexes of high nuclearity via controlled hydrolysis has been reported.[17,18] However, the methodology used yielded only in one case a dinuclear lanthanide core. Hydroxo complexes are also often proposed as intermediates in the degradation pathways of f-element organometallic[19] and coordination[20] compounds, and there are several reports of structurally characterized dinuclear hydroxo complexes of lanthanides usually obtained from nonaqueous solutions as the result of serendipitous hydrolysis.[16,21−24] However, general synthetic procedures for the preparation of dinuclear hydroxo complexes are lacking, and the reaction conditions and pathways that lead to the hydroxo formation in nonaqueous solvents are rarely elucidated.[25] Moreover, the ease in which lanthanide complexes are able to undergo hydrolysis in the presence of stoichiometric amounts of water is often underestimated especially in the presence of neutral basic ligands such as unhindered podands containing aromatic N-donors.

In the past few years we have been studying the coordination properties of such ligands, in particular the tripod tris(2-pyridylmethyl)amine (tpa; Chart 1) with trivalent lanthanides and trivalent uranium.[26,27] Polydentate oligoamines are of interest for their selective recognition of actinides with respect to lanthanides and have been demonstrated to be attractive ancillary ligands for the development of uranium(III) coordination chemistry.[26,28,29] Furthermore, the use of chiral tpa derivatives leads to lanthanide complexes which can act as anion-specific luminescent sensors.[30,31] Ln(III) complexes of the tetrapodal analogue N-donor ligand *N*,*N*,*N*′,*N*′-tetrakis(2-pyridylmethyl)ethylenediamine have also shown a high stability and a good efficiency for the catalytic hydrolysis of RNA.[32] In previous studies we have shown that the reaction of lanthanide(III) chloride salts with tpa in methanol only leads to the formation of mono(tpa) complexes, while proton NMR studies show that the reaction of iodide salts of lanthanum in anhydrous acetonitrile results in the formation of mono- or bis(tpa) complexes depending on the reaction stoichiometry.[26,27] In this Article we report the syntheses in anhydrous conditions and the solid-state structures of a series of bis(tpa) Ln(III) complexes and describe the reactivity of both mono- and bis(tpa) complexes with water, which leads to the systematic preparation of dinuclear hydroxo complexes.

Experimental Section

General Details. ^{1}H NMR spectra were recorded on Bruker AM-400 and Varian U-400 spectrometers in CD_3CN with CH_3CN as the internal standard. CD_3CN was vacuum distilled from CaH_2 after a 72 h reflux. Elemental analyses of the complexes were performed under argon by Analytische Laboratorien GmbH at Lindlar, Germany.

All manipulations of the lanthanide complexes were carried out under an inert argon atmosphere using Schlenk techniques and a Braun glovebox equipped with a purifier unit (unless otherwise stated). The water and oxygen levels were always maintained at less than 1 ppm. The solvents were purchased from Aldrich in their anhydrous forms, were transferred into a Schlenk flask under argon, and were vacuum distilled from K (diisopropyl ether) or CaH_2 (acetonitrile). Starting materials were purchased from Aldrich, Fluka, and Alfa and used without further purification unless otherwise stated. Anhydrous beads of LnI_3 (Ln = La(III), Ce(III), Nd(III), Lu(III)) were purchased from Aldrich. [$LnI_3(thf)_n$] salts (Ln = La(III), Ce(III), $n = 4$; Ln = Nd(III), Lu(III), $n = 3.5$)[33,34] were prepared by stirring overnight anhydrous LnI_3 in thf. The white (La, Ce, Lu) or pale blue (Nd) powders obtained after filtration were purified by extraction in hot thf to give microcrystalline solids (80−90% yield). $M(OTf)_3$ (Ln = La(III), Ce(III), Nd(III), Eu(III), Lu(III)) salts were purchased from Aldrich. Residual water present in these salts was removed by heating at 180 °C under vacuum (10^{-2} mmHg) for two weeks. The ligand tpa was prepared according to the literature procedure.[35] ^{1}H NMR spectra of all the lanthanide complexes were recorded, and the values of the chemical shifts are given in Table 1. All of the ^{1}H NMR resonances of the lanthanide complexes were assigned by ^{1}H−^{1}H 2D COSY experiments.

Iodide Complexes. Preparation of [Ce(tpa)I_3] (1). A solution of $CeI_3(thf)_4$ in MeCN (30 mg, 0.037 mmol, 0.4 mL) was added to a stirred solution of tpa in MeCN (10.8 mg, 0.037 mmol, 0.3 mL). After 20 min of agitation, ^{i}Pr$_2$O (2 mL) was carefully layered onto the MeCN solution. After six weeks, the precipitated crystalline solid was collected by filtration, washed with minimal amounts of cold MeCN, and dried under reduced pressure to afford [Ce(tpa)I_3] in 56% yield, 17 mg. Suitable single crystals were obtained by heating a solution of the complex to 60 °C, and subsequently cooling to ambient temperature. Anal. Calcd for [Ce(tpa)I_3],

(17) Roesky, P. W.; Bürgstein, M. R. *Angew. Chem., Int. Ed.* **2000**, *39*, 549−551.
(18) Zheng, Z. *Chem. Commun.* **2001**, 2521−2529.
(19) Evans, W. J.; Hozbor, M. A.; Bott, S. G.; Robinson, G. H.; Atwood, J. L. *Inorg. Chem.* **1988**, *27*, 1990−1993.
(20) Domingos, A.; Elsegood, M. R. J.; Hillier, A. C.; Lin, G.; Liu, S. Y.; Lopes, I.; Marques, N.; Maunder, G.; McDonald, R.; Sella, A.; Steed, J. W.; Takats, J. *Inorg. Chem.* **2002**, *41*, 6761−6768.
(21) Wong, W. K.; Zhang, L. L.; Xue, F.; Mak, T. C. W. *J. Chem. Soc., Dalton Trans.* **1999**, 3053−3062.
(22) Grillone, M. D.; Benetollo, F.; Bompieri, G. *Polyhedron* **1991**, 2171−2177.
(23) Evans, W. J.; Rabe, G. W.; Ziller, J. W. *Inorg. Chem.* **1994**, *33*, 3072−3078.
(24) Wang, R.; Zhao, J.; Jin, T.; Xu, G.; Zhou, Z.; Zhou, X. *Polyhedron* **1998**, *17*, 43−47.
(25) He, H.; Zhu, X.; Hou, A.; Guo, J.; Wong, W.-K.; Wong, W.-Y.; Li, K.-F.; Cheah, K.-W. *Dalton Trans.* **2004**, 4064−4073.
(26) Wietzke, R.; Mazzanti, M.; Latour, J.-M.; Pecaut, J.; Cordier, P.-Y.; Madic, C. *Inorg. Chem.* **1998**, *37*, 6690−6697.
(27) Wietzke, R.; Mazzanti, M.; Latour, J.-M.; Pécaut, J. *J. Chem. Soc., Dalton Trans.* **2000**, 4167−4173.
(28) Karmazin, L.; Mazzanti, M.; Gateau, C.; Hill, C.; Pécaut, J. *Chem. Commun.* **2002**, 2892−2893.
(29) Karmazin, L.; Mazzanti, M.; Pécaut, J. *Inorg. Chem.* **2003**, *42*, 5900−5908.
(30) Yamada, T.; Shinoda, S.; Tsukube, H. *Chem. Commun.* **2002**, 1218−1219.
(31) Yamada, T.; Shinoda, S.; Sugimoto, H.; Uenishi, J.-i.; Tsukube, H. *Inorg. Chem.* **2003**, *42*, 7932−7937.
(32) Yashiro, M.; Ishikubo, A.; Takarada, T.; Komiyama, M. *Chem. Lett.* **1995**, *8*, 665−666.
(33) Izod, K.; Liddle, S. T.; Clegg, W. *Inorg. Chem.* **2004**, *43*, 214−218.
(34) Giesbrecht, G. R.; Gordon, J. C.; Clark, D. L.; Scott, B. L. *Inorg. Chem.* **2004**, *43*, 1065−1070.
(35) Anderegg, G.; Wenk, F. *Helv. Chim. Acta* **1967**, *50*, 2330−2332.

Table 1. ^{1}H Chemical Shifts of tpa Complexes in CD_3CN (Anhydrous Conditions) at 298 K and 400 MHz

complex	H_6	H_5	H_4	H_3	H_a, H_b	OH
$[La(tpa)I_3]$	8.38 (d)	7.33 (t)	8.01 (t)	7.67 (d)	4.70 (s)	
$[La(tpa)(OTf)_3]$	8.82 (d)	7.30 (m)	7.78 (t)	7.30 (m)	4.35 (s)	
$[La(tpa)(OTf)_3]^a$	8.78 (d)	7.33 (m)	7.81 (t)	7.33 (m)	4.30 (s)	
$[La(tpa)_2]I_3$	8.24 (d)	7.20 (t)	7.89 (td)	7.54 (d)	4.53 (s)	
$[La(tpa)_2][(OTf)_3]$	8.20 (d)	7.16 (t)	7.87 (t)	7.48 (d)	4.41 (s)	
$[La(tpa)(OH)]_2[(OTf)_4]$	8.75 (d)	7.33 (t)	7.61 (t)	7.11 (d)	4.14 (s)	
$[Ce(tpa)I_3]$	4.75 (br)	6.87 (d)	8.57 (t)	9.45 (d)	7.07 (br)	
$[Ce(tpa)(H_2O)_2I_3]$	5.10 (br)	6.72 (s)	8.19 (t)	8.78 (d)	7.10 (br)	3.89 (br)
$[Ce(tpa)(OTf)_3]$	5.01 (br)	7.47 (t)	6.03 (d)	7.70 (d)	3.45 (br)	
$[Ce(tpa)(OTf)_3]^a$	5.82 (br)	7.44 (t)	7.83 (d)	8.65 (d)	5.25 (br)	
$[Ce(tpa)_2]I_3$	−2.53 (br)	4.95 (d)	7.99 (t)	10.48 (d)	13.56 (br)	
$[Ce(tpa)_2][(OTf)_3]$	−1.02 (br)	4.99 (d)	7.60 (t)	9.86 (d)	13.68 (br)	
$[Ce(tpa)(OH)]_2I_4^b$	4.98 (br)	6.90 (d)	8.50 (t)	9.33 (d)	7.19 (s)	16.05 (br)
$[Nd(tpa)I_3]^b$	−1.16 (br)	5.67 (d)	7.90 (s)	10.65 (s)	15.45 (br)	
$[Nd(tpa)(OTf)_3]$	8.83 (br)	7.79 (d)	8.33 (t)	7.88 (d)	9.09 (br)	
$[Nd(tpa)(OTf)_3]^a$	9.24 (br)	9.12 (d)	8.31 (t)	7.74 (d)	7.16 (br)	
$[Nd(tpa)_2]I_3^b$	−2.79 (br)	5.21 (s)	7.71 (s)	10.96 (s)	17.64 (br)	
$[Nd(tpa)_2][(OTf)_3]^b$	−1.16 (br)	5.67 (d)	7.90 (s)	10.65 (s)	15.45 (br)	
$[Eu(tpa)(OTf)_3]$	5.83 (s)	5.43 (s)	6.96 (s)	4.51 (s)	−2.45 (s)	
$[Eu(tpa)(OTf)_3]^a$	6.43 (s)	5.62 (s)	6.93 (t)	4.31 (d)	−3.28 (s)	
$[Eu(tpa)(OTf)_3]^c$	7.30 (s)	7.76 (s)	8.39 (s)	7.51 (s)	3.90 (s)	
$[Eu(tpa)_2][(OTf)_3]$	31.69 (br)	11.63/0.64 (s)	9.83	0.64/11.63 (s)	−24.24, −37.30 (br)	
$[Eu(tpa)(OH)]_2[(OTf)_4]^b$	11.41 (br)	7.42 (d)	6.84 (t)	2.57 (d)	−7.19 (s)	
$[Eu(tpa)(OH)]_2[(OTf)_4]^c$	7.28 (s)	7.76 (s)	8.39 (s)	7.51 (s)	3.89 (s)	
$[Lu(tpa)I_3]$	9.26 (d)	7.61 (m)	8.06 (t)	7.61 (m)	4.75 (s)	
$[Lu(tpa)(OTf)_3]$	8.87 (d)	7.42 (m)	7.90 (td)	7.42 (m)	4.44 (s)	
$[Lu(tpa)(OTf)_3]^a$	8.78 (d)	7.43 (m)	7.91 (t)	7.43 (m)	4.43 (s)	
$[Lu(tpa)_2]I_3^b$	7.67 (br)	7.12 (t)	8.01 (td)	7.76 (d)	4.90 (s)	
$[Lu(tpa)_2][(OTf)_3]^b$	7.70 (br)	7.10 (t)	8.01 (t)	7.56 (d)	4.80 (s)	
$[Lu(tpa)(OH)]_2[(OTf)_4]$	8.44 (br)	7.16 (t)	7.77 (t)	7.34 (d)	4.40 (s)	

[a] Spectrum recorded in the presence of water. [b] Spectrum recorded at 343 K. [c] Spectrum recorded in D_2O.

$C_{18}H_{18}N_4CeI_3$: C, 26.55; H, 2.24; N, 6.91. Found: C, 26.52; H, 2.18; N, 7.03.

Preparation of $[La(tpa)_2]I_3$ (2). A solution of $LaI_3(thf)_4$ in MeCN (30 mg, 0.037 mmol, 1.5 mL) was added to a stirred solution of tpa in MeCN (21.7 mg, 0.074 mmol, 1.5 mL). After 30 min of agitation, $^iPr_2O$ (3 mL) was carefully layered onto the MeCN solution. After seven weeks, the crystals that resulted were collected by filtration, washed with minimal amounts of cold MeCN, and dried under reduced pressure to afford $[La(tpa)_2]I_3$ in 56% yield, 23 mg. Anal. Calcd for $[La(tpa)_2]I_3$, $C_{36}H_{36}N_8LaI_3$: C, 39.25; H, 3.27; N, 10.18. Found: C, 39.55; H, 3.38; N, 10.33.

$[M(tpa)_2]I_3$. A solution of $MI_3(thf)_4$ (M = Ce(III), Nd(III), Lu(III)) in MeCN (0.037 mmol, 1.5 mL) was layered onto a MeCN solution of tpa (0.074 mmol, 1.5 mL) and the resulting layered solution left to stand for 3 weeks. After this time, the resultant crystals were collected by filtration, washed with minimal amounts of cold MeCN, and dried under reduced pressure to afford yellow (Ce), pale green (Nd), or colorless (Lu) crystals of the $[M(tpa)_2]I_3$ complexes in 70−80% yield.

$[Ce(tpa)_2]I_3$ (3). Anal. Calcd for $[Ce(tpa)_2]I_3$, $C_{36}H_{36}N_8CeI_3$: C, 39.25; H, 3.29; N, 10.17. Found: C, 39.20; H, 3.32; N, 10.20. ES-MS (MeCN, *m*/*z*): $\{Ce(tpa)_2I_2\}^+$, 973.5; $\{Ce(tpa)I_2\}^+$, 683.9; $\{Ce(tpa)_2I\}^{2+}$, 423.5.

$[Nd(tpa)_2]I_3$ (4). Anal. Calcd for $[Nd(tpa)_2]I_3$, $C_{36}H_{36}N_8NdI_3$: C, 39.10; H, 3.28; N, 10.13. Found: C, 39.13; H, 3.34; N, 10.25.

$[Lu(tpa)_2]I_3$ (5). Anal. Calcd for $[Lu(tpa)_2]I_3$, $C_{36}H_{36}N_8LuI_3$: C, 38.05; H, 3.19; N, 9.86. Found: C, 38.22; H, 3.31; N, 9.91.

Triflate Complexes. Acetonitrile solutions (10^{-2} M) of $[M(tpa)_2][(OTf)_3]$ complexes for NMR and ES-MS studies were prepared in situ by reaction of the triflate salts with tpa in a ratio of 1:2 under rigorously anhydrous conditions. All chemical shifts for the triflate complexes are given in Table 1. As a representative example of the lanthanide series, only the europium bis(tpa) triflate complex was isolated and fully characterized.

Preparation of $[Eu(tpa)_2][(OTf)_3]$ (6). A suspension of $Eu(OTf)_3$ in 3 mL of MeCN (30 mg, 0.05 mmol) was added slowly to a stirred MeCN solution containing a slight excess of tpa (32.0 mg, 0.11 mmol, 2 mL). After being stirred for 16 h, the solution was filtered and reduced in volume to 2 mL, and 6 mL of $^iPr_2O$ was added. After diffusion was complete (about two weeks), the crystalline solid that resulted was isolated by filtration, washed with minimal amounts of MeCN, and dried by vacuum suction to yield $[Eu(tpa)_2][(OTf)_3]$ as a white microcrystalline powder in 40% yield, 24 mg. Anal. Calcd for $[Eu(tpa)_2][(OTf)_3]\cdot 0.25MeCN\cdot 0.25H_2O$, $C_{39.5}H_{37.25}O_{9.25}N_{8.25}S_3F_9Eu$: C, 39.72; H, 3.12; N, 9.67. Found: C, 39.47; H, 3.29; N, 9.70.

Synthesis of $[Eu(tpa)(OTf)_3(H_2O)_2]$ (7). In air, a solution of tpa (24.4 mg, 0.083 mmol) in MeCN (nondistilled) (2 mL) was added to a stirred suspension of $Eu(OTf)_3$ (50 mg, 0.083 mmol) in MeCN (3 mL). After being stirred for 14 h, the solution was filtered and reduced in volume to 3 mL, and 8 mL of $^iPr_2O$ was added. After diffusion was complete (about two weeks), the microcrystalline precipitate was isolated by filtration, washed with minimal amounts of MeCN, and dried under reduced pressure to yield $[Eu(tpa)(OTf)_3(H_2O)_2]$ as a white powder in 66% yield, 51 mg. Single crystals suitable for diffraction analysis were grown by slow vapor diffusion of $^iPr_2O$ into a 2×10^{-2} M MeCN solution of the complex. ES-MS (MeCN, *m*/*z*): $\{[Eu(tpa)(OTf)_2]\}^+$, 740.9. Anal. Calcd for $[Eu(tpa)(OTf)_3(H_2O)_2]$, $C_{21}H_{22}O_{11}N_4S_3F_9Eu$: C, 27.25; H, 2.40; N, 6.05. Found: C, 27.10; H, 2.32; N, 6.19.

^{1}H NMR of Monoprotonated tpa, [Htpa(OTf)]. NMR (400 MHz, CD_3CN, 298 K): δ_H 8.55 (d, 3H, $^3J_{HH}$ = 4.4 Hz, H_6), 7.79 (t, 3H, $^3J_{HH}$ = 6.8 Hz, H_4), 7.49 (d, 6H, $^3J_{HH}$ = 7.6 Hz, H_3), 7.13, (t, 3H, $^3J_{HH}$ = 7.6 Hz, H_5) 4.10 (s, 6H, H_a, H_b).

Hydroxo Complexes. Preparation of $[Eu(tpa)(\mu\text{-}OH)(OTf)_2]_2$ (8). A solution of $Eu(OTf)_3$ in MeCN (50 mg, 0.083 mmol, 3.0 mL) was added to a stirred solution of tpa in MeCN (49 mg, 0.167 mmol, 3.0 mL). After the resulting solution was stirred for 48 h, 2

equiv of a 0.5 M H_2O solution in MeCN (0.167 mmol, 330 μL) was added dropwise by syringe and the resulting solution stirred for a further 24 h. Subsequent addition of another 2 equiv of H_2O, followed by stirring for 24 h and recrystallization from MeCN/^{i}Pr$_2$O (1:3), afforded [Eu(tpa)(μ-OH)(OTf)$_2$]$_2$ as a microcrystalline white solid in 76% yield, 96 mg. Single crystals suitable for diffraction analysis were grown by slow diffusion of ^{i}Pr$_2$O into a 2×10^{-2} M MeCN solution of the complex. ES-MS (MeCN, *m*/*z*): {[Eu(tpa)(OH)]$_2$[(OTf$_3$]}$^+$, 1364.4 (87); {Eu(tpa)(OTf)$_2$}$^+$, 740.9 (3); {[Eu(tpa)(OH)]$_2$(OTf)$_2$]}$^{2+}$, 608 (100). ES-MS (H_2O, *m*/*z*): {[Eu(tpa)(OTf)$_2$]}$^+$, 740.9 (100); {[Eu(tpa)(OH)(OTf)]}$^+$, 609 (89); {[Eu(tpa)(OH)]$_2$[(OTf$_3$]}$^+$, 1364.4 (7); {[Eu(tpa)$_2$(OTf)$_2$]$_2$}$^+$, 1030.3 (46). Anal. Calcd for [Eu(tpa)(OH)(OTf)$_2$]$_2$, $C_{40}H_{38}O_{14}S_4F_{12}N_8Eu_2$: C, 31.71; H, 2.53; N, 7.40. Found: C, 31.55; H, 2.49; N, 7.52.

Acetonitrile and deuterated acetonitrile solutions of [Ln(tpa)(μ-OH)(OTf)$_2$]$_2$ (Ln = La, Lu) complexes for ES-MS and NMR spectroscopy were prepared in situ with the procedure described above for the europium complex. ES-MS (MeCN, *m*/*z*): M$^+$, {[La(tpa)(OH)]$_2$[(OTf$_3$]}$^+$, 1338.3 (43); {M − H_2O}$^+$, 1320.7 (3); {[La(tpa)(OTf)$_2$]}$^+$, 726.9 (17); {M − OTf}$^{2+}$, 594.7 (46); {[La(tpa)$_2$(OTf)]}$^{2+}$, 434.0 (42); {[La(tpa)$_2$(OTf)$_2$]}$^+$, 1016.5 (14). ES-MS (MeCN, *m*/*z*): M$^+$, {[Lu(tpa)(OH)]$_2$[OTf]$_3$}$^+$, 1410.7 (33); {M − H_2O}$^+$, 1392.8 (14); {M − OTf}$^{2+}$, 630.9 (11).

Preparation of [Ce(tpa)(OH)(MeCN)(H_2O)]$_2$I$_4$ (9). A solution of CeI$_3$(thf)$_4$ in MeCN (100 mg, 0.124 mmol, 5.0 mL) was added to a stirred solution of tpa in MeCN (72 mg, 0.248 mmol, 5.0 mL). After 1 h of agitation, 2 equiv of a 0.5 M H_2O solution in MeCN (0.248 mmol, 490 μL) was added dropwise by syringe and the resulting solution stirred for a further 24 h. Subsequent addition of another 2 equiv of H_2O, followed by stirring for 24 h and recrystallization from MeCN/^{i}Pr$_2$O (1:3), afforded [Ce(tpa)(μ-OH)(MeCN)(H_2O)]$_2$I$_4$ as a microcrystalline yellow solid in 48% yield, 45 mg. Single crystals suitable for diffraction analysis were grown by slow diffusion of ^{i}Pr$_2$O into a 2×10^{-2} M MeCN solution of the complex. Anal. Calcd for [Ce(tpa)(μ-OH)(MeCN)(H_2O)]$_2$I$_4$, $C_{40}H_{48}O_4N_{10}Ce_2I_4$: C, 31.59; H, 3.18; N, 9.21. Found: C, 31.35; H, 3.01; N, 9.34.

Mass Spectrometry. The mass spectra were acquired on an LCQ ion trap (Thermo Electron, San Jose, CA), equipped with an electrospray source. Electrospray full scan spectra, in the range of *m*/*z* 50−2000 amu, were obtained by infusion through fused silica tubing at 2−10 μL min^{-1}. The solutions were analyzed in positive mode. The LCQ calibration (*m*/*z* 50−2000) was achieved according to the standard calibration procedure from the manufacturer (mixture of caffeine, MRFA, and Ultramark 1621). The temperature of the heated capillary of the LCQ was set to the range of 80−160 °C; the ion spray voltage was in the range of 1−7 kV with an injection time of 5−200 ms.

X-ray Crystallography. All diffraction data were taken using a Bruker SMART CCD area detector three-circle diffractometer (Mo Kα radiation, graphite monochromator, λ = 0.71073 Å). To prevent hydrolysis, the crystals were coated with a light hydrocarbon oil and quickly transferred to a stream of cold nitrogen on the diffractometer.

The cell parameters were obtained with intensities detected on 3 batches of 15 frames. The crystal−detector distance was 5 cm. For three settings of ϕ and 2θ, narrow data frames were collected with 0.3° increments in ω. A full hemisphere of data were collected for **3**, **5**, **6**, **7**, **8**, and **9**, and a quadrant of data were collected for **1**, **2**, and **4**. At the end of the data collection, the first 50 frames were re-collected to establish that crystal decay had not taken place during the collection. Unique intensities with $I > 10\sigma(I)$ detected on all frames using the Bruker SMART program[36] were used to refine the values of the cell parameters. The substantial redundancy in data allows empirical absorption corrections to be applied using multiple measurements of equivalent reflections with the SADABS Bruker program.[36] Space groups were determined from systematic absences, and they were confirmed by the successful solution of the structure (Table 2). Complete information on the crystal data and data collection parameters are given in the Supporting Information.

The structures were solved by direct methods using the SHELXTL 6.10 package,[37] and all atoms (including all hydrogen atoms for complexes **1** and **3**−**8** and hydrogens of the coordinated hydroxo and water molecule in **9**) were found by difference Fourier syntheses. Hydrogen atoms for complexes **2** and **9** were included in calculated positions and thermal parameters refined isotropically. All non-hydrogen atoms were anisotropically refined on F^2. The comparison of M−N and M−O bond lengths in a series of crystal structures of isostructural lanthanide complexes allows an uncertainty estimation of ~0.008 Å for the measured values of the M−N distances, indicating that differences in bond distances larger than 0.025 Å are significant.

Results and Discussion

Lanthanide Complexation with tpa. The reaction of the lanthanide salts LnI$_3$(thf)$_4$ (Ln = La(III), Nd(III), Ce(III), Lu(III)) and Ln(OTf)$_3$ (Ln = La(III), Ce(III), Eu(III), Lu(III)) with tpa in rigorously anhydrous conditions was followed by proton NMR spectroscopy.

The proton NMR spectra of 1:1 solutions of LnI$_3$(thf)$_4$ and tpa in CD$_3$CN (10^{-2} M) (Ln = La(III), Nd(III), Ce(III), Lu(III)) show the presence of a single species with four resonances for the pyridine protons and a single resonance for the methylene protons which have been assigned to the 1:1 complexes of tpa. To confirm this assignment, the cerium complex has been isolated, and single crystals suitable for X-ray analysis were obtained by heating a solution of the complex to 60 °C for 1 h and subsequently cooling to ambient temperature. The crystal structure of [Ce(tpa)I$_3$] (**1**) is shown in Figure 1, and selected interatomic distances and angles are given in Table 3. The Ce cation is seven coordinate with a slightly distorted capped octahedral coordination geometry. The atoms N(2), N(3), I(2), and I(3) occupy the equatorial plane, the remaining iodide and pyridine N occupy the axial coordination sites, and the apical N atom (N(4)) occupies the capping position. The observed values of the Ce−N distances (2.614(3)−2.71(4) Å) are similar to those found in the related complex [CeI$_2$(terpy)$_2$]$^+$ (2.614(3)−2.662(2) Å).[38] The tetradentate tpa adopts a helicoidal pseudo-C_3-symmetric arrangement. In contrast to the previously reported adducts [M(tpa)I$_3$(py)] (M = La, U)[27] isolated from pyridine solution, which are eight coordinate, **1** does not contain a solvent molecule coordinated to the metal center in the solid state.

The proton NMR spectrum of **1** is consistent with a solution structure in which all three chelating arms of the

(36) Bruker, Madison, WI, 1995.
(37) Sheldrick, G. M. *SHELXTL 6.10*, 5th ed.; University of Göttingen: Göttingen, Germany, 1994.
(38) Berthet, J.-C.; Rivière, C.; Miquel, Y.; Nierlich, M.; Madic, C.; Ephritikhine, M. *Eur. J. Inorg. Chem.* **2002**, 1439−1446.

Table 2. Crystallographic Data for the Nine Structures of Complexes **1**−**9**

	1	**2**·3MeCN	**3**·3MeCN	**4**·3MeCN	**5**·3MeCN
empirical formula	$C_{18}H_{18}CeI_3N_4$	$C_{42}H_{45}N_{11}I_3La$	$C_{42}H_{45}N_{11}I_3Ce$	$C_{42}H_{45}N_{11}I_3Nd$	$C_{42}H_{45}N_{11}I_3Lu$
fw	811.18	1223.50	1224.71	1228.83	1259.56
cryst syst	monoclinic	orthorhombic	orthorhombic	orthorhombic	orthorhombic
space group	*P*2(1)/*n*	*P*2(1)2(1)2(1)	*P*2(1)2(1)2(1)	*P*2(1)2(1)2(1)	*P*2(1)2(1)2(1)
a, Å	9.4958(19)	12.041(2)	12.004(2)	11.945(2)	11.909(2)
b, Å	14.668(3)	18.151(4)	18.072(4)	17.952(4)	17.745(4)
c, Å	16.946(3)	22.217(4)	22.267(5)	22.335(5)	22.510(5)
β, deg	101.19(3)				
V, Å^3; *Z*	2315.4(8); 4	4855.7(17); 4	4830.4(17); 4	4789.7(17)	4757.0(16)
D_{calcd}, g cm^{-3}	2.327	1.674	1.684	1.704	1.759
μ(Mo Kα), mm^{-1}	5.975	2.827	2.900	3.058	4.063
temp, K	223(2)	223(2)	223(2)	223(2)	223(2)
R1, wR2[a]	0.0340, 0.0882	0.0638, 0.1466	0.0308, 0.0587	0.0461, 0.0934	0.0259, 0.0577
Flack param		0.01(3)	0.01(1)	0.02(2)	0.028(6)

	6·0.5MeCN·0.08H_2O	**7**	**8**	**9**·2MeCN
empirical formula	$C_{40}H_{37.65}EuF_9N_{8.50}O_{9.08}S_3$	$C_{21}H_{22}EuF_9N_4O_{11}S_3$	$C_{40}H_{38}Eu_2F_{12}N_8O_{14}S_4$	$C_{44}H_{54}Ce_2I_4N_{12}O_4$
fw	1201.80	925.57	1514.94	1602.84
cryst syst	monoclinic	triclinic	triclinic	monoclinic
space group	*P*2(1)/*c*	*P*$\bar{1}$	*P*$\bar{1}$	*P*2(1)/*n*
a, Å	19.057(3)	10.486(1)	10.168(2)	15.058(9)
b, Å	21.469(4)	11.584(2)	10.759(2)	12.077(7)
c, Å	23.605(4)	13.948(2)	13.117(3)	15.880(9)
α, deg		74.694(3)	101.038(3)	
β, deg	90.065(3)	88.535(2)	101.996(3)	102.835(9)
γ, deg		76.139(2)	106.494(3)	
V, Å^3; *Z*	9657(3); 8	1585.4(4); 2	1296.9(4); 1	2816(3); 2
D_{calcd}, g cm^{-3}	1.653	1.939	1.940	1.891
μ(Mo Kα), mm^{-1}	1.525	2.290	2.671	3.838
temp, K	193(2)	223(2)	223(2)	223(2)
R1, wR2[a]	0.0283, 0.0644	0.0210, 0.0501	0.0204, 0.0551	0.0673, 0.1783

[a] The structures were refined on F_o^2 using all data: wR2 = $[\sum[w(F_o^2 - F_c^2)^2]/\sum w(F_o^2)^2]^{1/2}$, where $w^{-1} = [\sum(F_o^2) + (aP)^2 + bP]$ ($P = [\max(F_o^2, 0) + 2F_c^2]/3$).

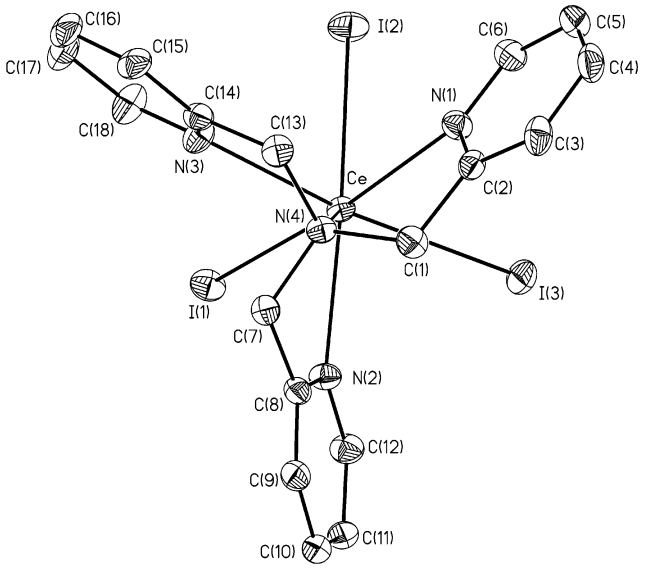

Figure 1. Molecular structure of the complex [Ce(tpa)I_3] (**1**) with thermal ellipsoids at 30% probability.

ligand are equivalent on the NMR time scale. The presence of a single signal for the methylene protons indicates that the complex displays a dynamically averaged C_{3v} structure at room temperature.

Similarly the proton NMR spectra of 1:2 solutions of LnI_3-(thf)$_4$ and tpa in CD_3CN (10^{-2} M) show the presence of a single species with four resonances for the pyridine protons and a single resonance for the methylene protons indicative of a dynamically averaged D_{3h} structure at room temperature.

Table 3. Selected Bond Lengths (Å) and Angles (deg) in the Complex [Ce(tpa)I_3] (**1**)

Ce−N(4)	2.615(3)	Ce−I(3)	3.1022(7)
Ce−N(3)	2.619(4)	Ce−I(2)	3.1161(8)
Ce−N(2)	2.646(4)	Ce−I(1)	3.1447(8)
Ce−N(1)	2.671(4)		
N(4)−Ce−N(3)	63.09(12)	N(3)−Ce−I(2)	82.58(9)
N(4)−Ce−N(2)	63.91(11)	N(2)−Ce−I(2)	169.27(8)
N(3)−Ce−N(2)	100.56(13)	N(1)−Ce−I(2)	82.06(8)
N(4)−Ce−N(1)	62.24(12)	I(3)−Ce−I(2)	93.907(15)
N(3)−Ce−N(1)	94.58(13)	N(4)−Ce−I(1)	124.54(9)
N(2)−Ce−N(1)	107.75(12)	N(3)−Ce−I(1)	85.71(9)
N(4)−Ce−I(3)	115.57(9)	N(2)−Ce−I(1)	80.12(9)
N(3)−Ce−I(3)	173.53(10)	N(1)−Ce−I(1)	171.89(8)
N(2)−Ce−I(3)	83.88(9)	I(3)−Ce−I(1)	99.75(2)
N(1)−Ce−I(3)	79.52(9)	I(2)−Ce−I(1)	89.942(18)
N(4)−Ce−I(2)	126.03(7)		

These signals have been assigned to the 2:1 complexes of tpa, which have been isolated and characterized by X-ray diffractometry. For Ce and Nd, the pyridine resonances are considerably paramagnetically shifted and broadened at room temperature, indicative of a geometrical change compared to the mono(tpa) analogues.

^{1}H NMR titrations between LnI_3(thf)$_4$ and tpa in anhydrous acetonitrile under argon show the successive formation of the mono- and bis(tpa) complexes on addition of 1 and 2 equiv of ligand, respectively (the titration for Ce is shown in Figure 2a,b). Upon addition of an excess (3−4 equiv) of tpa, the spectra show only resonances characteristic of [Ln(tpa)$_2$]I_3 and free tpa; the spectra remain unchanged after several weeks.

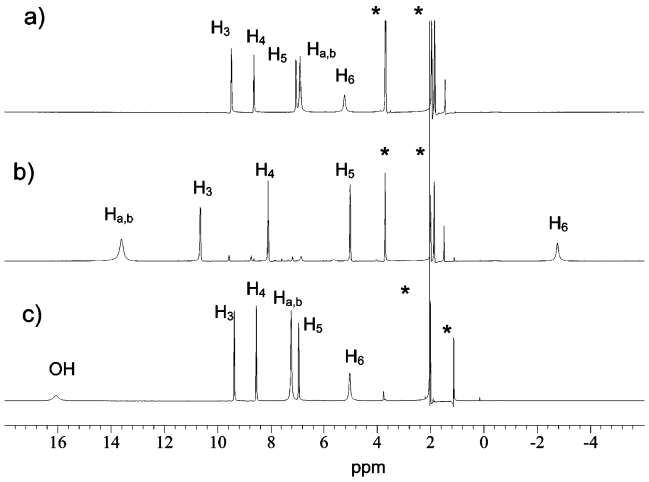

Figure 2. ^{1}H NMR in CD_3CN under argon at 298 K of (a) a 1:1 mixture of tpa and CeI_3.4thf, (b) a 2:1 mixture of tpa and CeI_3.4thf, and (c) [Ce(tpa)(μ-OH)(MeCN)(H_2O)]$_2I_4$. The asterisks denote diamagnetic solvent resonances.

Analogously to the iodide salts, ^{1}H NMR titrations of CD_3CN solutions of $Ln(OTf)_3$ (Ln = La(III), Ce(III), Eu(III), and Lu(III)) with tpa (1−2 equiv) under rigorously anhydrous conditions show the successive formation of two species on addition of 1 and 2 equiv of ligand. Electrospray mass spectrometry measurements performed on the bis(tpa) triflate complexes $[Ln(tpa)_2][(OTf)_3]$ (Ln = La, Lu, 10^{-3} M) show the presence of a molecular ion peak: $[La(tpa)_2(OTf)_2]^+$, *m*/*z* 1016.5 (relative intensity 29); $[Lu(tpa)_2(OTf)_2]^+$, *m*/*z* 1052.1 (relative intensity 15). The formulation of these species as mono- and bis(tpa) complexes, respectively, was confirmed by a single-crystal X-ray diffraction study of the europium derivatives (see below).

Similarly to the iodide systems, addition of a third ligand equivalent results in spectra showing only two sets of signals assigned to $[Ln(tpa)_2][(OTf)_3]$ complexes and free tpa; again the spectra remain unchanged after several weeks. These results show that, while the use of lanthanide chloride salts only leads to the formation of mono(tpa) complexes, the employment of the less coordinating iodide and triflate anions yields bis(tpa) complexes (for a metal:ligand ratio of 1:2). However, only bis(tpa) complexes are formed even in the presence of a large excess of tpa in contrast to a recent report describing the formation of tris(tpa) complexes with triflate salts of lanthanum upon addition of 3 equiv of tpa. In our hands, we find no evidence of the formation of an additional compound under anhydrous conditions.

Crystal Structure of Bis(tpa) Complexes. $[Ln(tpa)_2]I_3$ complexes were prepared for Ln = La(III), Ce(III), Nd(III), and Lu(III) by treating tpa with $LnI_3(thf)_4$ in anhydrous acetonitrile under argon in a stoichiometric ratio of 2:1. The $[Ln(tpa)_2]I_3$ compounds were isolated in reasonable yields from concentrated acetonitrile solutions ($\sim 10^{-2}$ M) or by addition of isopropyl ether (La). Large crystals suitable for X-ray diffraction were obtained for all complexes under these conditions. The complexes $[Ln(tpa)_2]I_3$ (Ln = La(III) (**2**), Ce(III) (**3**), Nd(III) (**4**), Lu(III) (**5**)) are both isostructural to one another and to the solid-state structure of $[U(tpa)_2]I_3$ previously reported.[29] Accordingly only the crystal structure

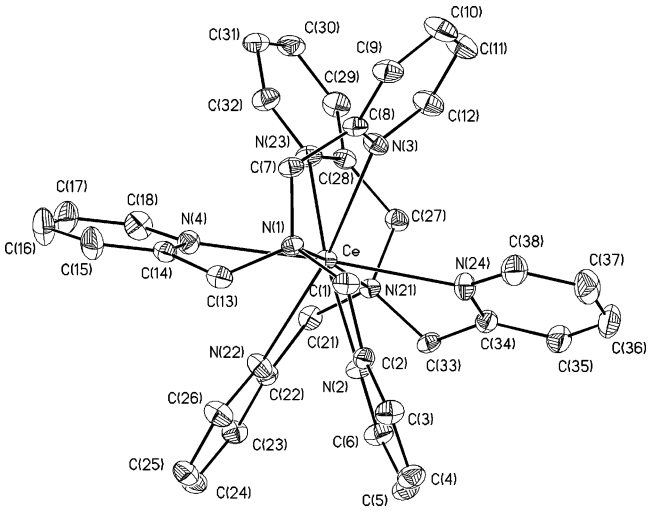

Figure 3. ORTEP diagram of the cation $[Ce(tpa)_2]^+$ in complex **3** with thermal ellipsoids at 30% probability.

Table 4. Selected Bond Lengths (Å) and Angles (deg) in the Complexes $[Ln(tpa)_2]I_3$ (**2**−**5**)

	$[La(tpa)_2]I_3$ (**2**)	$[Ce(tpa)_2]I_3$ (**3**)	$[Nd(tpa)_2]I_3$ (**4**)	$[Lu(tpa)_2]I_3$ (**5**)
M−N(3)	2.629(9)	2.608(4)	2.581(4)	2.465(3)
M−N(22)	2.634(8)	2.619(3)	2.587(4)	2.479(4)
M−N(2)	2.644(8)	2.610(3)	2.574(4)	2.469(4)
M−N(1)	2.651(8)	2.620(3)	2.586(4)	2.487(4)
M−N(23)	2.653(8)	2.626(4)	2.598(4)	2.484(3)
M−N(21)	2.654(9)	2.621(3)	2.590(4)	2.490(3)
M−N(24)	2.680(7)	2.666(3)	2.615(4)	2.514(3)
M−N(4)	2.700(7)	2.665(3)	2.617(4)	2.511(4)
N(3)−M−N(22)	86.4(3)	85.89(11)	84.03(12)	80.85(12)
N(3)−M−N(2)	98.6(3)	98.48(11)	99.34(12)	101.52(12)
N(22)−M−N(2)	75.9(3)	75.43(11)	74.62(12)	72.55(12)
N(3)−M−N(1)	101.1(3)	101.36(11)	102.31(12)	104.83(13)
N(22)−M−N(1)	172.2(3)	172.27(11)	173.07(12)	173.76(12)
N(2)−M−N(1)	104.9(3)	105.81(11)	106.73(13)	108.30(13)
N(3)−M−N(23)	173.6(3)	174.15(11)	174.76(13)	176.08(14)
N(22)−M−N(23)	100.0(3)	99.91(12)	101.05(12)	102.84(13)
N(2)−M−N(23)	82.3(3)	82.34(11)	80.98(13)	78.55(12)
N(1)−M−N(23)	72.6(3)	72.88(12)	72.67(13)	71.54(13)
N(3)−M−N(21)	74.8(3)	74.68(11)	73.74(12)	72.30(11)
N(22)−M−N(21)	99.6(3)	99.72(11)	100.18(12)	103.04(12)
N(2)−M−N(21)	172.4(3)	172.05(12)	171.93(12)	173.12(12)
N(1)−M−N(21)	80.4(3)	79.86(11)	79.19(13)	76.68(13)
N(23)−M−N(21)	104.7(3)	104.88(11)	106.30(12)	107.82(12)
N(3)−M−N(24)	120.9(3)	120.65(10)	119.70(11)	117.13(11)
N(22)−M−N(24)	63.2(2)	63.57(10)	64.16(12)	65.85(11)
N(2)−M−N(24)	118.6(2)	118.48(10)	117.29(12)	115.48(13)
N(1)−M−N(24)	110.4(2)	109.84(10)	109.75(12)	108.75(11)
N(23)−M−N(24)	63.5(2)	63.35(10)	64.25(12)	66.00(12)
N(21)−M−N(24)	63.4(2)	63.39(10)	64.39(12)	66.15(11)
N(3)−M−N(4)	64.2(3)	64.18(10)	64.76(12)	66.32(11)
N(22)−M−N(4)	123.3(2)	123.14(10)	122.16(12)	119.54(11)
N(2)−M−N(4)	63.4(2)	63.87(10)	65.00(12)	66.77(12)
N(1)−M−N(4)	62.8(2)	63.28(10)	63.81(12)	65.80(11)
N(23)−M−N(4)	111.0(2)	111.42(10)	110.99(12)	110.36(12)
N(21)−La−N(4)	115.6(2)	115.32(10)	114.30(12)	112.27(12)
N(24)−La−N(4)	172.9(2)	172.89(10)	173.37(11)	174.47(11)

of **3** is shown in Figure 3, and selected interatomic distances and angles are given for all complexes in Table 4. The metal ions are eight coordinate by the two tetradentate ligands that wrap around the metal in a pseudo-D_3-symmetric arrangement. All the complexes crystallize as a single enantiomer in the noncentrosymmetric space group $P2_12_12_1$. The coordination geometries are best described as distorted cubes, where N(1), N(21), N(3), and N(4) describe one square base,

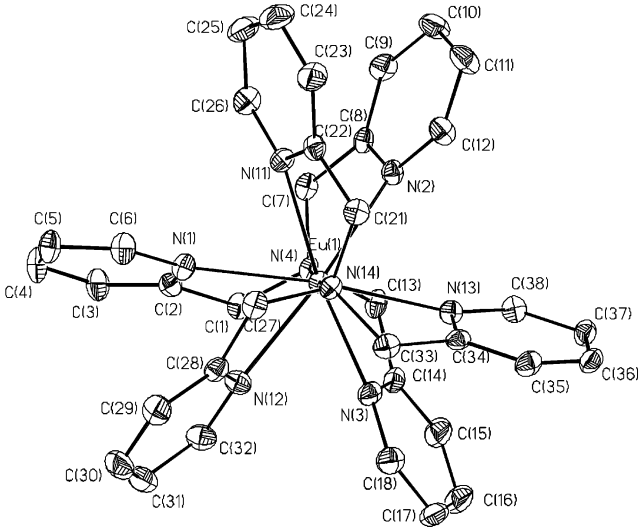

Figure 4. ORTEP diagram of the cation $[Eu(tpa)_2]^{3+}$ in **6** with thermal ellipsoids at 30% probability.

and N(2), N(22), N(23), and N(24) occupy the opposing square plane. The angle between the two faces decreases with decreasing ionic radius (5.6° for La, 5.3° for Ce, 4.6° for Nd, and 3.8° for Lu), resulting in a less distorted polyhedron for Lu. The Ln−N bond distances also show a general linear increase with increasing ionic radius as expected in a purely ionic bonding model for ligands that can adapt well to differently sized metals. However, the previously reported nitrogen−uranium bond distances are shorter than expected on the basis of this model, with a Δd(M−N) between La and U of 0.031 Å (decrease expected from the variation of the ionic radii, 0.007 Å).[39] Although this difference lies just outside the limits of the significance criterion (0.025 Å) and is only slightly higher than the one observed for the mono(tpa) adducts [M(tpa)(py)I_3] (0.025 Å), it could reflect a stronger metal−ligand interaction for uranium. A lower Δd(M−N) between La and U had been observed for the complexes of the "harder" tripodal ligand bis(Mentb) (Mentb = tris(*N*-methylbenzimidazol-2-ylmethyl)amine) derivatives (0.016 Å).[27]

The europium triflate bis(tpa) complex was also isolated from an anhydrous acetonitrile solution by addition of isopropyl ether to confirm the structure formulation for the triflates. While it was not possible to obtain crystals suitable for X-ray diffraction under rigorously anhydrous conditions, single crystals of $[Eu(tpa)_2][(OTf)_3]$ (**6**) were isolated in the presence of <0.5 equiv of water. The crystal structure of **6** is shown in Figure 4, and selected interatomic distances and angles are given in Table 5. The molecular structure of **6** is essentially identical to those of the bis(tpa) iodides. Differently from these complexes, **6** crystallizes in a centrosymmetric space group with two molecules of complex per asymmetric unit cell and 0.15 molecule of water, which presumably aids the crystallization process. The mean value of the Eu−N distances (2.54(1) Å) is slightly shorter than the value found in the seven-coordinate chloride complex [Eu(tpa)Cl_3] (2.58(2) Å).[26]

(39) Shannon, R. D. *Acta Crystallogr.* **1976**, *A32*, 751−767.

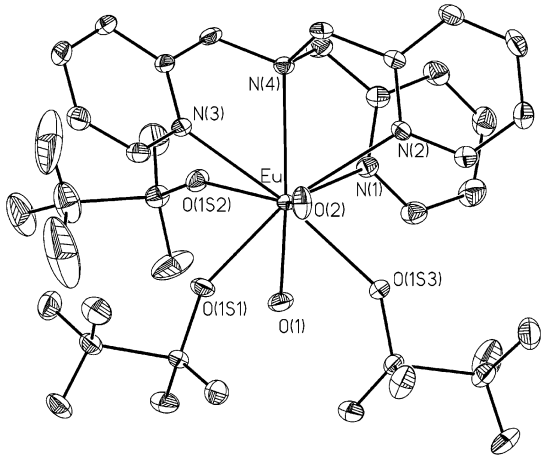

Figure 5. ORTEP diagram of the complex $[Eu(tpa)(OTf)_3(H_2O)_2]$ (**7**) with thermal ellipsoids at 30% probability.

Table 5. Selected Bond Lengths (Å) and Angles (deg) in the Complex $[Eu(tpa)_2](OTf)_3$ (**6**)

Eu1−N3	2.522(3)	Eu1−N11	2.548(3)
Eu1−N2	2.525(3)	Eu1−N4	2.554(3)
Eu1−N12	2.528(3)	Eu1−N14	2.560(3)
Eu1−N13	2.535(3)	Eu1−N1	2.564(3)
N3−Eu1−N2	101.54(10)	N11−Eu1−N4	112.35(9)
N3−Eu1−N12	84.00(10)	N3−Eu1−N14	117.93(9)
N2−Eu1−N12	174.41(9)	N2−Eu1−N14	112.63(9)
N3−Eu1−N13	72.63(9)	N12−Eu1−N14	64.73(9)
N2−Eu1−N13	80.52(9)	N13−Eu1−N14	64.50(9)
N12−Eu1−N13	102.06(9)	N11−Eu1−N14	64.48(9)
N3−Eu1−N11	172.77(9)	N4−Eu1−N14	176.58(9)
N2−Eu1−N11	71.52(9)	N3−Eu1−N1	102.54(9)
N12−Eu1−N11	102.98(9)	N2−Eu1−N1	104.36(9)
N13−Eu1−N11	103.68(9)	N12−Eu1−N1	73.41(9)
N3−Eu1−N4	65.05(9)	N13−Eu1−N1	173.90(9)
N2−Eu1−N4	64.49(9)	N11−Eu1−N1	81.53(9)
N12−Eu1−N4	117.96(9)	N4−Eu1−N1	3.97(8)
N13−Eu1−N4	115.98(9)	N14−Eu1−N1	115.95(9)

Hydroxo Complexes of tpa. Proton NMR titrations of CD_3CN solutions of $Ln(OTf)_3$ (Ln = La(III), Ce(III), Nd(III), Eu(III), and Lu(III)) with tpa (1−2 equiv) in the presence of water led to the reproduction of the data recently reported by Tsukube and co-workers.[31] The spectra show the formation of one species upon the addition of 0−1 equiv of tpa, assigned to the mono(tpa) complexes. The chemical shifts of the complexed ligand protons are slightly displaced with respect to those in anhydrous conditions in agreement with the presence of coordinated water molecules. Indeed, single crystals of the bis(aqua) complex $[Eu(tpa)(OTf)_3(H_2O)_2]$ (**7**) were isolated by slow diffusion of $^iPr_2O$ into a saturated MeCN solution of the complex. The crystal structure of **7** is shown in Figure 5, and selected interatomic distances and angles are given in Table 6. The metal ion is nine coordinate, and the coordination geometry can be described as a capped square antiprism, with the three triflate oxygens and one pyridyl nitrogen (N1) forming one face (deviation from the mean plane 0.083 Å) and the tpa nitrogens N2, N3, and N4 and one water oxygen forming the opposite face (deviation from the mean plane 0.035 Å). The Eu−N distances (2.575(3)−2.682(3) Å) are slightly longer than those found in the eight-coordinate bis(tpa) complex (2.513(3)−2.574(3) Å). The capping position is occupied by one water molecule, and the angle between the

Table 6. Selected Bond Lengths (Å) and Angles (deg) in the Complex $[Eu(tpa)(OTf)_3(H_2O)_2]$ (**7**)

Eu−O(1S2)	2.383(2)	Eu−N(1)	2.575(3)
Eu−O(2)	2.417(3)	Eu−N(4)	2.628(2)
Eu−O(1S1)	2.428(2)	Eu−N(3)	2.642(3)
Eu−O(1S3)	2.449(2)	Eu−N(2)	2.682(3)
Eu−O(1)	2.462(3)		
O(1S2)−Eu−O(2)	140.91(10)	O(1S3)−Eu−N(4)	134.61(8)
O(1S2)−Eu−O(1S1)	85.99(9)	O(1)−Eu−N(4)	128.21(10)
O(2)−Eu−O(1S1)	72.27(10)	N(1)−Eu−N(4)	66.64(8)
O(1S2)−Eu−O(1S3)	138.16(8)	O(1S2)−Eu−N(3)	70.61(8)
O(2)−Eu−O(1S3)	74.12(9)	O(2)−Eu−N(3)	72.27(9)
O(1S1)−Eu−O(1S3)	87.13(8)	O(1S1)−Eu−N(3)	73.82(8)
O(1S2)−Eu−O(1)	69.79(10)	O(1S3)−Eu−N(3)	145.04(8)
O(2)−Eu−O(1)	129.98(11)	O(1)−Eu−N(3)	129.67(9)
O(1S1)−Eu−O(1)	73.64(9)	N(1)−Eu−N(3)	127.56(8)
O(1S3)−Eu−O(1)	68.66(9)	N(4)−Eu−N(3)	62.94(8)
O(1S2)−Eu−N(1)	81.03(9)	O(1S2)−Eu−N(2)	133.45(8)
O(2)−Eu−N(1)	133.00(10)	O(2)−Eu−N(2)	66.68(9)
O(1S1)−Eu−N(1)	147.88(8)	O(1S1)−Eu−N(2)	137.71(8)
O(1S3)−Eu−N(1)	83.34(8)	O(1S3)−Eu−N(2)	72.57(8)
O(1)−Eu−N(1)	74.32(9)	O(1)−Eu−N(2)	127.63(9)
O(1S2)−Eu−N(4)	71.64(8)	N(1)−Eu−N(2)	67.39(8)
O(2)−Eu−N(4)	101.70(9)	N(4)−Eu−N(2)	64.90(8)
O(1S1)−Eu−N(4)	135.72(8)	N(3)−Eu−N(2)	102.16(8)

two faces is 0.6°. The pseudo-C_3-symmetric arrangement of the tpa ligand observed in the cerium iodide complex **1** and in the complex $[Eu(tpa)Cl_3]$ is disrupted by the inversion of the orientation of one pyridyl ring.

On addition of 2 equiv of tpa, ^{1}H NMR spectroscopy shows the complete disappearance of the signals of the mono(tpa) complex and the presence of two new sets of signals, one of which was unambiguously assigned to protonated tpa.[29,40] Increasing additions of tpa (up to 3 equiv) did not result in the formation of additional species. Electrospray mass spectra allowed us to identify the species formed for La, Eu, and Lu as dimeric hydroxo complexes of tpa (molecular ion peak corresponding to $([M_2(tpa)_2(OH)_2(OTf)_3]^+$) with *m*/*z* 1410.9 for Lu, *m*/*z* 1338.3 for La, and *m*/*z* 1364 for Eu (Figure 6). The molecular ion peak of protonated tpa is also observed at *m*/*z* 291.1. The ESI-MS spectra indicate that the hydroxo complexes retain their dimeric structure in acetonitrile solution. In the case of Eu, diffusion of ^{i}Pr$_2$O into the 1:3 metal/ligand mixture results in the precipitation of this complex, the structure of which was determined by X-ray crystallography, affording the formulation $[Eu(tpa)(\mu\text{-OH})(OTf)_2]_2$ (**8**). The crystal structure of **8** is shown in Figure 7, and selected interatomic distances and angles are given in Table 7. In complex **8** two $[Eu(tpa)(OH)(OTf)_2]$ moieties are joined by two bridging hydroxides to form a centrosymmetric dimer. Each europium is eight coordinate, and its coordination environment can be viewed as a distorted dodecahedron. The tetradentate ligand tpa occupies four adjacent corners of the dodecahedron, the remaining sites being occupied by two triflate anions acting as unidentate ligands and by the two bridging hydroxides. The Eu−N distances vary only slightly with respect to those of complex **7** despite the difference in coordination number. The dimer is formed by sharing the edge O(1)−O(1A) of the dodecahedron formed by each half of the molecule. The

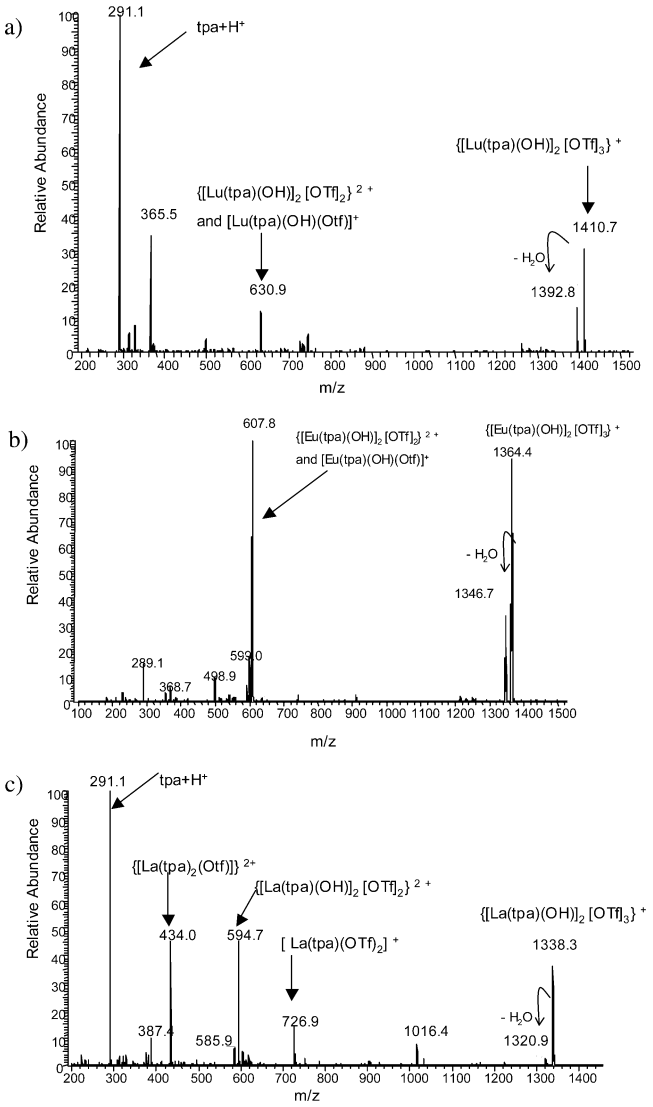

Figure 6. ES-MS spectra of 1:2 acetonitrile solutions of $Ln(OTf)_3$ ($\sim 10^{-3}$ M) and tpa (Ln = La (c), Lu (a)) and of the isolated hydroxo complex $[Eu(tpa)(\mu\text{-OH})(OTf)_2]_2$ (b).

pyridyl arms of the ligand adopt a fanlike nonsymmetrical arrangement similar to that found in complex **7**.

The isolation of **8** confirms that, in the presence of water, the coordinated water molecules of the parent mono(tpa) complex are deprotonated by the addition of an excess of tpa to yield a dimeric hydroxo complex according to eq 1. Interestingly, NMR and ES-MS spectra indicate that the hydrolysis reaction does not go further on addition of a large excess of tpa and water (up to 6 equiv).

$$2[Eu(tpa)(OTf)_3(H_2O)_2] + 2tpa \rightarrow [Eu(tpa)(\mu\text{-OH})(OTf)_2]_2 + 2H_2O + 2tpaH(OTf) \quad (1)$$

In the presence of stoichiometric amounts of water the formation of bis(tpa) complexes is not observed. Conversely, the tpa ligand ($pK_{a1} = 6.17$, $pK_{a2} = 4.35$, $pK_{a3} = 2.55$) reacts as a base with the acidic coordinated water molecules. A similar reactivity has also been observed with the less basic tripod tris(2-pyrazinylmethyl)amine ($pK_a = 3$).[41]

(40) Hazell, A.; McGinley, J.; Toftlund, H. *J. Chem. Soc., Dalton Trans.* **1999**, 1271−1276.

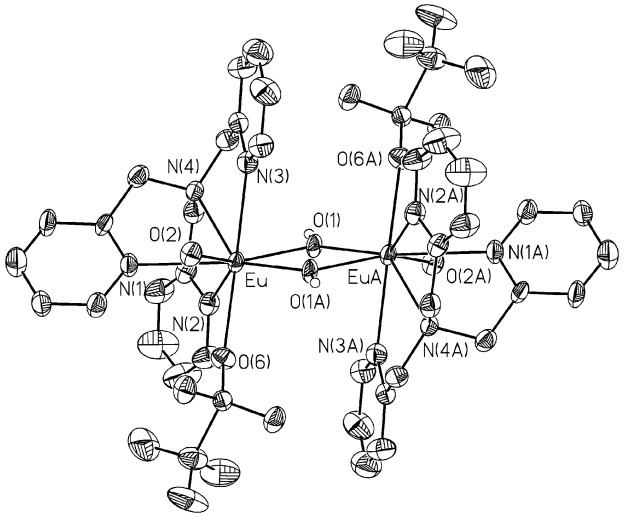

Figure 7. ORTEP diagram of the complex $[Eu(tpa)(\mu\text{-}OH)(OTf)_2]_2$ (**8**) with thermal ellipsoids at 30% probability (several atoms of the triflates (O(2) and O(2A)) were omitted for clarity).

Table 7. Selected Bond Lengths (Å) and Angles (deg) in the Complex $[Eu(tpa)(\mu\text{-}OH)(OTf)_2]_2$ (**8**)[a]

Eu−O(1)	2.228(2)	Eu−N(2)	2.593(3)
Eu−O(1)#1	2.298(2)	Eu−N(4)	2.639(2)
Eu−O(1S2)	2.381(2)	Eu−N(3)	2.730(3)
Eu−O(1S1)	2.531(2)	Eu#1−O(1)	2.298(2)
Eu−N(1)	2.578(3)	Eu−Eu#1	3.7153(8)
O(1)−Eu−O(1)#1	69.64(10)	O(1)−Eu−N(4)	82.12(8)
O(1)−Eu−O(1S2)	109.11(8)	O(1)#1−Eu−N(4)	136.86(8)
O(1)#1−Eu−O(1S2)	84.89(8)	O(1S2)−Eu−N(4)	136.28(8)
O(1)−Eu−O(1S1)	144.84(8)	O(1S1)−Eu−N(4)	117.75(8)
O(1)#1−Eu−O(1S1)	76.85(8)	N(1)−Eu−N(4)	66.07(8)
O(1S2)−Eu−O(1S1)	77.43(8)	N(2)−Eu−N(4)	64.60(8)
O(1)−Eu−N(1)	142.33(8)	O(1)−Eu−N(3)	80.72(8)
O(1)#1−Eu−N(1)	148.01(8)	O(1)#1−Eu−N(3)	136.28(8)
O(1S2)−Eu−N(1)	83.44(8)	O(1S2)−Eu−N(3)	75.08(8)
O(1S1)−Eu−N(1)	71.58(7)	O(1S1)−Eu−N(3)	133.07(8)
O(1)−Eu−N(2)	89.19(8)	N(1)−Eu−N(3)	68.13(8)
O(1)#1−Eu−N(2)	82.57(8)	N(2)−Eu−N(3)	129.50(8)
O(1S2)−Eu−N(2)	152.55(8)	N(4)−Eu−N(3)	65.03(8)
O(1S1)−Eu−N(2)	75.98(8)	Eu−O(1)−Eu#1	110.36(10)
N(1)−Eu−N(2)	94.51(8)		

[a] Symmetry transformations used to generate equivalent atoms: #1, $-x+2, -y+1, -z+1$.

The complex $[Eu(tpa)(\mu\text{-}OH)(OTf)_2]_2$ was also prepared in a controlled manner by slow addition of a stoichiometric amount of water to a solution of the bis(tpa) complex in anhydrous acetonitrile according to eq 2. The complex was obtained in 76% yield, and its purity was established by NMR spectroscopy and elemental analysis.

$$2[Eu(tpa)_2(OTf_3)] + 2H_2O \rightarrow [Eu(tpa)(\mu\text{-}OH)(OTf)_2]_2 + 2tpaH(OTf) \quad (2)$$

The mechanism for this reaction is likely to involve displacement of one tpa ligand by two water molecules to form the mono(tpa) complex, which will subsequently react with the noncoordinated tpa, affording the dimeric hydroxo complex. In agreement with this mechanism, no bis(tpa) reaction intermediates were observed by ^{1}H NMR spectroscopy. Furthermore, only the formation of bisligand complexes was observed for the related tripodal ligand tris(2-benzimidazolylmethyl)amine (ntb) in the presence of a ligand excess despite its basic character. In the bis(ntb) complexes, the formation of bisligand species is highly favored by strong intramolecular $\pi-\pi$ electrostatic interactions, leading to a K_2/K_1 value >1.[42] These results indicate that the formation of hydroxide species is hampered when the bisligand complex is highly stable with respect to ligand dissociation. The ES-MS spectra of the isolated hydroxo complex of europium in water show a principal peak corresponding to ($[Eu(tpa)(OH)(OTf)]^+$) (m/z 608), indicating that the dimer can dissociate in water. A small peak corresponding to the dimeric species is however also observed in water. A partial dissociation of the ligand is also observed by NMR and ES-MS spectroscopy in water.

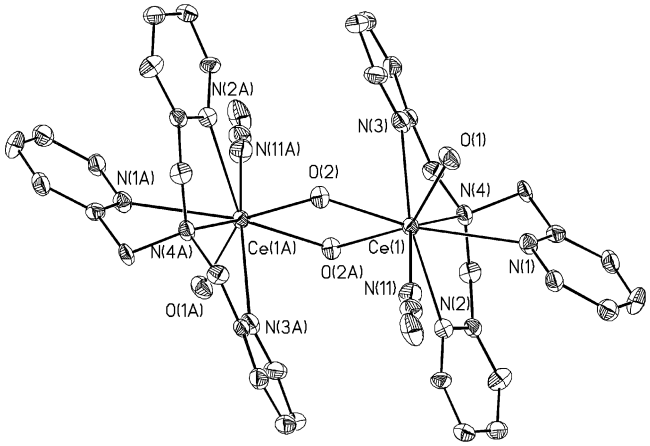

Figure 8. ORTEP diagram of the cation $[Ce(tpa)(\mu\text{-}OH)(MeCN)(H_2O)]_2^{4+}$ in **9** with thermal ellipsoids at 30% probability.

Addition of a 0.1 M solution of H_2O in MeCN (2 equiv) to a solution of $[Ce(tpa)_2]I_3$ in anhydrous acetonitrile (followed by NMR spectroscopy, Figure 2c) also resulted in the complete conversion of the complex into a new paramagnetic species accompanied by the formation of protonated tpa (eq 3). The nature of the resultant hydroxo

$$[Ce(tpa)_2]I_3 + 2H_2O \rightarrow {}^1/_2[Ce(tpa)(\mu\text{-}OH)(MeCN)(H_2O)]_2I_4 + tpaHI \quad (3)$$

product $[Ce(tpa)(\mu\text{-}OH)(MeCN)(H_2O)]_2I_4$ (**9**) was confirmed by X-ray diffraction analysis. The complex was isolated in reasonable yield by addition of diisopropyl ether to an acetonitrile solution of **9**.

Single crystals of **9** were grown by slow diffusion of ^{i}Pr$_2$O into an acetonitrile solution of the complex. The crystal structure of **9** in which two identical moieties, [Ce(tpa)(OH)-(MeCN)(H_2O)], are joined by two μ-hydroxide groups to form a centrosymmetric dimer is shown in Figure 8, and selected interatomic distances and angles are given in Table 8. In **9** each metal ion is eight coordinate and presents a distorted dodecahedral coordination geometry with an arrangement of the tetradentate tpa and the hydroxide ligands

(41) Wietzke, R. *CEA*; Université Joseph Fourier-Grenoble I: Grenoble, France, 1999.

(42) Wietzke, R.; Mazzanti, M.; Latour, J.-M.; Pécaut, J. *J. Chem. Soc., Chem. Commun.* **1999**, 209−210.

Table 8. Selected Bond Lengths (Å) and Angles (deg) in the Complex $[Ce(tpa)(\mu\text{-}OH)(MeCN)(H_2O)]_2I_4$ (**9**)[a]

Ce(1)−O(2)#1	2.324(7)	Ce(1)−N(11)	2.667(11)
Ce(1)−O(2)	2.337(7)	Ce(1)−N(1)	2.676(9)
Ce(1)−O(1)	2.516(8)	Ce(1)−N(4)	2.690(8)
Ce(1)−N(3)	2.630(9)	Ce(1)#1−O(2)	2.324(7)
Ce(1)−N(2)	2.653(9)	Ce(1)−Ce(1)#1	3.829(2)
O(2)#1−Ce(1)−O(2)	69.5(3)	O(2)#1−Ce(1)−N(1)	137.9(3)
O(2)#1−Ce(1)−O(1)	146.1(3)	O(2)−Ce(1)−N(1)	152.4(2)
O(2)−Ce(1)−O(1)	80.5(3)	O(1)−Ce(1)−N(1)	74.0(3)
O(2)#1−Ce(1)−N(3)	81.6(3)	N(3)−Ce(1)−N(1)	102.8(3)
O(2)−Ce(1)−N(3)	82.4(3)	N(2)−Ce(1)−N(1)	67.1(3)
O(1)−Ce(1)−N(3)	79.1(3)	N(11)−Ce(1)−N(1)	83.9(3)
O(2)#1−Ce(1)−N(2)	76.8(3)	O(2)#1−Ce(1)−N(4)	79.8(3)
O(2)−Ce(1)−N(2)	131.2(3)	O(2)−Ce(1)−N(4)	136.9(3)
O(1)−Ce(1)−N(2)	136.8(3)	O(1)−Ce(1)−N(4)	115.0(3)
N(3)−Ce(1)−N(2)	126.7(3)	N(3)−Ce(1)−N(4)	63.4(3)
O(2)#1−Ce(1)−N(11)	112.1(3)	N(2)−Ce(1)−N(4)	65.1(3)
O(2)−Ce(1)−N(11)	79.7(3)	N(11)−Ce(1)−N(4)	141.5(3)
O(1)−Ce(1)−N(11)	76.2(3)	N(1)−Ce(1)−N(4)	66.1(2)
N(3)−Ce(1)−N(11)	151.5(3)	Ce(1)#1−O(2)−Ce(1)	110.5(3)
N(2)−Ce(1)−N(11)	81.6(3)		

[a] Symmetry transformations used to generate equivalent atoms: #1, $-x+2, -y+1, -z+1$.

analogous to that of complex **8**, the main difference from the europium complex **8** being the presence of one molecule of water and one molecule of acetonitrile in the remaining coordination sites, while the iodide anions act as noncoordinating counterions. This structural difference can be interpreted in terms of the lower coordinating ability of iodides with respect to triflates. The Ce−O (OH) (2.337(7) and 2.324(7) Å) and the Ce···Ce′ (3.829(2) Å) distances are similar to those reported for the bismethoxo complex $[(Me_3CC_5H_4)_2Ce_2(\mu\text{-}OCHMe)]_2$ (Ce−O = 2.373(3) and 2.369(3) Å; Ce···Ce′ = 3.844(2) Å).[43]

Similarly to the formation of **8**, reaction 3 probably involves substitution of one tpa ligand by two water molecules to form the mono-tpa complex which will subsequently react with the non coordinated tpa to yield the dimeric hydroxo complex. Indeed, complex **9** was also obtained as the only product when excess tpa was added to a solution of $Ce(tpa)I_3$ initially treated with two equivalents of water.

The previously described reaction (eq 4) of the bis(tpa) complex of trivalent uranium with water resulted in the formation of an oxo complex of tetravalent uranium.[29] The

$$[U(tpa)_2]I_3 + H_2O \rightarrow {}^1/_3\{[U(tpa)(\mu\text{-}O)I]_3(\mu\text{-}I)\}I_2 + {}^1/_2H_2 + \text{tpaHI} \quad (4)$$

suggested mechanism invoked a uranium(IV) hydroxo complex as the reaction intermediate. The different reactivities shown by cerium and uranium arise from the difference in the oxidation potentials of the two cations: that of the U(IV)/U(III) couple is −0.63 V in aqueous solution, while that of the Ce(IV)/Ce(III) couple is +1.74 V.[44]

Conclusion

The solid-state and solution structural studies described in this Article show very different results for the complexation of lanthanides with the neutral tripodal N-donor ligand tpa depending on the experimental conditions used. In rigorously anhydrous conditions, two tpa ligands displace the coordinated solvent and counterions (triflates or iodides) to form bisligand lanthanide complexes in which the metal ion is only coordinated by neutral N-donors.

In the presence of water, the coordinated water molecules of the parent mono(tpa) complex are deprotonated by the addition of excess tpa, affording a dimeric hydroxo complex and protonated tpa. Under these conditions the formation of bis(tpa) complexes was never observed.

This study shows that the presence of small amounts of water in organic solvents greatly affects the complexation studies of lanthanides in the presence of neutral N-donor ligands.

Furthermore, in this Article we describe a facile synthetic route to a family of discrete dimeric hydroxo-bridged lanthanide complexes prepared in a controlled manner; work toward extending this chemistry to other ligands is currently in progress. Such dimeric hydroxo species are good starting materials for the synthesis of larger oxo/hydroxo lanthanide clusters and represent synthetic models that mimic the dinuclear active site of metallophosphodiesterases.

Acknowledgment. This work was supported by the Commissariat à l'Energie Atomique, Direction de l'Energie Nucléaire. We thank Pierre-Alain Bayle for help with the NMR experiments and Christelle Gateau for the synthesis of the ligand tpa.

Supporting Information Available: Figures S1 and S2 showing the proton NMR of titration of $Eu(OTf)_3$ with tpa and complete tables of crystal data and structure refinement, atomic coordinates, bond lengths and angles, anisotropic displacement parameters, and hydrogen coordinates for compounds **1**−**9**. This material is available free of charge via the Internet at http://pubs.acs.org.

IC0502224

(43) Stults, S. D.; Andersen, R. A.; Zalkin, A. *Organometallics* **1990**, *9*, 1623−1629.
(44) Johnson, D. A. *Some Thermodynamic Aspects of Inorganic Chemistry*, 2nd ed.; Cambridge University Press: Cambridge, U.K., 1982.